

A Sensitive Electrochemical Sensor Based on Graphene/Pt Nanoparticles for Simultaneous Determination of Tyrosine and Tryptophan in the Presence of 5-hydroxytryptophan

Yingliang Wei *, Anting Wang, Lu Wang

Department of Environmental Engineering and Chemistry, Luoyang Institute of Science and Technology, Luoyang, 471023, Henan Province, P. R. China

*E-mail: wei66720@126.com

Received: 29 January 2020 / Accepted: 11 September 2020 / Published: 31 October 2020

A composite material, namely, graphene/ Pt nanoparticles (GR/PtNPs) was prepared in this work. This composite material was characterized by transmission electron microscopy (TEM) and Fourier transform infrared spectroscopy (FTIR). Based on GR/PtNPs modified glassy carbon electrode (GR/PtNPs/GCE), a sensitive and simple sensor was developed for simultaneous measurement of tryptophan (Trp) and tyrosine (Tyr) in the presence of 5-hydroxytryptophan(5-HTP). Under optimized measurement conditions, the oxidation peak current of Tyr increased linearly within a concentration range from 5.0×10^{-7} to 2.0×10^{-5} mol/L with a detection limit of 1.25×10^{-7} mol/L. The linear response of Trp was also obtained in the range from 2.0×10^{-7} to 1.2×10^{-5} mol/L, and the detection limit was 8.22×10^{-8} mol/L. When Tyr and Trp samples were measured, the recovery rate of tyrosine was 98.4% to 103.5%, and the recovery rate of tryptophan was 98.7% to 102.9%, which indicates that the accuracy of GR/PtNPs/GCE was high. Additionally, the GR/ PtNPs/GCE demonstrated suitable selectivity for the determination of tryptophan (Trp) and tyrosine (Tyr), making it practicable for their measurement of Trp and Tyr in pharmaceutical formulations.

Keywords: Graphene; Sodium polystyrene sulfonate; Pt nanoparticles; Tyrosine; Tryptophan

1. INTRODUCTION

Tyrosine (Tyr) and tryptophan (Trp) are two kinds of essential amino acids in many biochemical processes for the human body. Tyr is the precursor of catecholamine synthesis such as dopamine and serotonin [1]. The unsuitable quantity of Tyr has distinct effect on some human diseases. High level of Tyr may lead to dementia or Parkinson's disease and the increase of sister chromatid exchange, while the absence of Tyr can cause depression, alkaptonuria [2]. Trp is an important amino acid for infants with normal growth and for adults who need to maintain nitrogen balance. The content

of Trp in plasma has a bearing on the extent of hepatic disease [3]. Therefore, it is significant to meet the measurement demand of Trp and Tyr in many fields such as pharmaceuticals, food production, and medical detection.

Several reports about the detection of Trp and Tyr have been published such as high-performance liquid chromatography (HPLC) [4], gas chromatography–mass spectrometry (GC–MS) [5], capillary electrophoresis (CE) [6], and spectrophotometry [7]. The above-mentioned methods need long analytical time and/or expensive, and sometime need the treatment before the detection. Owing to the desirable characteristic of electroanalytical method, such as simple operation, sensitivity, and accuracy, it has attracted much attention for the determination of Trp or Tyr in past years. For instance, A sensor based on Au-nanoparticles/poly-eriochrome black T film was developed for simultaneous determination of L-cysteine and L-tyrosine [8]. Functionalized graphene quantum dots with bi-metallic nanoparticles composite modified electrode was employed to determine ascorbic acid, dopamine, uric acid and tryptophan simultaneously [9]. Voltammetric method of simultaneous determination of tyrosine, acetaminophen and ascorbic acid has been reported [10]. Silver/graphene oxide nanocomposite was conveniently fabricated and used for the construction of a disposable electrochemical sensor for the determination of Trp [11]. However, simultaneous detection of Trp and Tyr in the existence of 5-hydroxytryptophan (5-HTP) by using GR/ PtNPs/GCE has not been reported.

GR displays its great potential application in ultrasensitive sensor and field-effect transistor, due to its excellent conductivity and chemical stability [12, 13]. In recent years, some novel electrodes modified with graphene have been developed to detect some biological molecules such as dopamine (DA), acetaminophen (ACOP), tyramine [14,15]. Polystyrene sodium sulfonate (PSS) is a polymer based on polystyrene with a benzene ring that contains SO_3^{2-} and Na^+ ions. PSS can strongly interact with GO by π - π accumulation, and therefore it would be used as a dispersant for suspension of graphitic nanoplatelets in aqueous solution [16]. Owing to high conductivity and high surface-to-volume ratio, precious metal nanoparticles have better catalytic characteristics compared with conventional particles [17]. Pt nanoparticles (PtNPs) have received much attention in catalysis and sensors because it can provide excellent catalytic activity and environment friendly for biological molecules [18]. In this work, a composite nano-material of GR/PtNPs was synthesized, and the as-prepared sensor was used for the measurement of Trp and Tyr in pharmaceutical formulations.

2. EXPERIMENTAL

2.1 Reagents and chemicals

Graphite was provided by Nanjing Xianfeng Nano-material Technology Company, China. Polystyrene sodium sulfonate (PSS) was purchased from Shanghai Xinping Fine Chemicals Company, China. Tyr, Trp and 5-HTP were bought from Shanghai Yuanye Biological Technology Company, China. Other reagents were of analytical grade without further purification. The water used in our experiment was redistilled water.

2.2 Apparatus

All electrochemical experiments were performed on a CHI 660D Electrochemical Analyzer (CH Instrument, USA). A three-electrode system was used, in which a modified glassy carbon electrode (GCE) was used as working electrode, a platinum wire as the counter electrode and a saturated calomel electrode (SCE) as reference electrode, respectively. All the potentials were reported vs. SCE. The measurements of pH value were carried out by a PHS-3C Digital pH-meter (Shanghai Yidian Science Instrument Company, Shanghai, China). Transmission electron microscopy (TEM) analysis was performed using a JEM 2100 microscope (Jeol Ltd., Japan). Fourier transform infrared (FTIR) spectra were recorded on a Tensor 27 Infrared spectrometer (Bruker Corporation, Germany). Chromatography assay was carried out with LC-2000 liquid Chromatograph (Shanghai Tianmei Instrument Company, China). All experiments were performed at the room temperature (25 ± 1 °C).

2.3 Development of composite modified electrode

Graphene oxide (GO) was synthesized from natural graphite using a modified Hummers method [19]. 20 mg GO was suspended in 20 mL water and sonicated for about 1 h to develop a homogeneous GO suspension. 200mg of PSS was dissolved in this suspension by sonication for 2 h, and then 0.8mL of 1% K_2PtCl_4 was added under stirring for about 2 h to obtain the mixture solution. Subsequently, 10 mL of 2 mg/mL $NaBH_4$ solution was added slowly into the above-mentioned mixture solution. The reaction was carried out at 60 °C for 24 h under stirring. The reaction product was centrifugated, and then dried overnight in vacuum drying box at 50 °C. Finally, GR/ PtNPs composite nano-material was obtained. 2.0 mg GR/ PtNPs was added to 4.0 mL redistilled water. This mixture ---was sonicated for 30 min in ultrasound bath to form a stable suspension.

Before modification, bare GCE was firstly polished mechanically with 0.5 μm and 0.05 μm alumina slurry, then rinsed and sonicated successively in HNO_3 - H_2O (v/v = 1:1), anhydrous ethanol and redistilled water. The appropriate amount of 0.5 mg/mL GR/PtNPs composite dispersion was coated on the pretreated GCE and dried at room temperature. Finally, GR/ PtNPs composite modified GCE (GR/ PtNPs/GCE) was fabricated successfully.

2.4 Analytical procedure

In the consequent experiments, GR/PtNPs/GCE was used as the working electrode. The three-electrode system was transferred into 10 mL pH=0.4 sodium sulfate- sulfuric acid solution containing an appropriate amount of Trp and Tyr. Voltammetric curves within the potential window of 0.2-1.1 V were recorded, and the oxidation peaks current (I_{pa}) were measured at 0.834 V for Trp and 0.936 V for Tyr, respectively. After each measurement, in order to clean out the previous residue completely, this modified electrode was refreshed by 10 cyclic voltammetric sweeps between 0.2 and 1.1 V with the scan rate of 50 mV/s in blank buffer solution.

3. RESULTS AND DISCUSSION

3.1 Characterization of GR/PtNPs

The morphology of GR/PtNPs was characterized by TEM, as shown in Figure 1. Figure 1a demonstrates there are many wrinkled nanosheets on the surface of GO. Owing to the presence of wrinkle, GO can display its high surface area, excellent electronic and chemical characteristics. Figure 1b illustrates TEM image of GR/PtNPs. The thickness of GR becomes thinner by the dispersion of PSS. Many observable dots due to the assembly of PtNPs were clearly observed. TEM image confirmed that GR/ PtNPs composite material has been synthesized successfully.

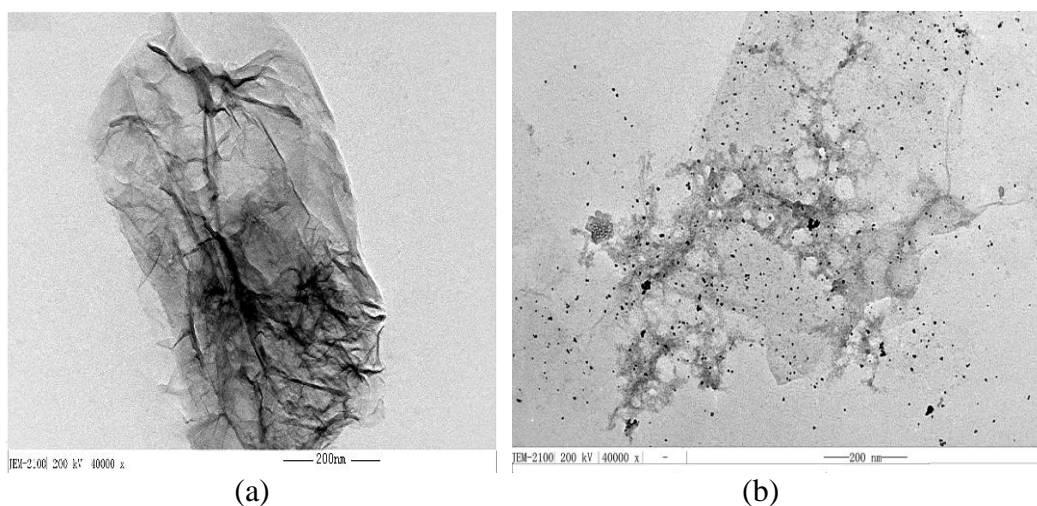


Figure 1. TEM images of GO (a) and GR/ PtNPs (b)

3.2 Characterization of GO and GR by FTIR

FTIR was also employed to study the structural changes for GO, GR and GR/PSS composite material, as shown in Figure 2. The characteristic peaks of the oxygen groups in GO such as the C=O stretching vibration peaks, the vibration peak of O-H bond, the stretching vibration peaks of epoxy and alkoxy C-O bonds were observed at 1725 cm^{-1} , 3390 cm^{-1} , 1225 cm^{-1} and 1046 cm^{-1} , respectively (curve a). Additionally, the typical stretching vibration peaks of C=C functional group at 1629 cm^{-1} was also observed. The reduction of GO is evidenced by dramatic decrease in peak intensity at 3390 , 1725 , 1225 cm^{-1} , and 1046 cm^{-1} (curve b), indicating that GO has been successfully reduced to GR. From FTIR spectrum of GR/PSS (curve c), the absorption peaks at 1170 , 1118 , 1025 cm^{-1} correspond to the stretching vibration for S=O and S-C functional group of PSS[20]. The weak peak at 830 cm^{-1} is due to the deformation vibration for parallel substitution of benzene ring. This experimental results demonstrate that GR/PSS composite material has synthesized successfully by the proposed method.

3.3 Characterization of GR/ PtNPs/GCE by electrochemical impedance spectroscopy

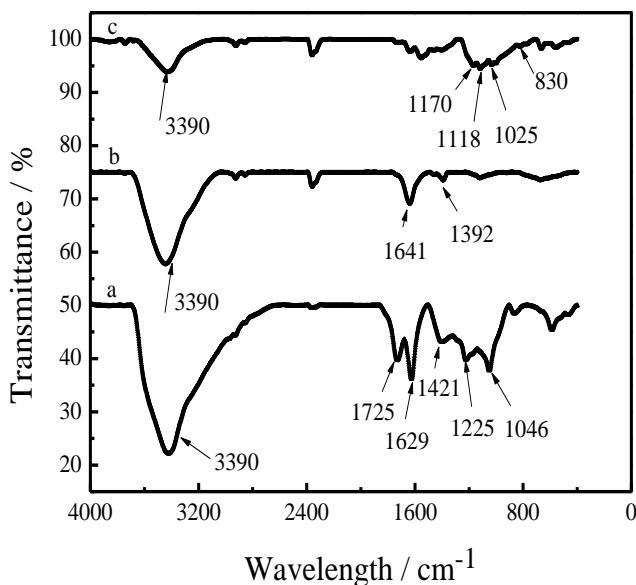


Figure 2. FTIR spectra of GO (a), GR (b) and GR/ PSS (c)

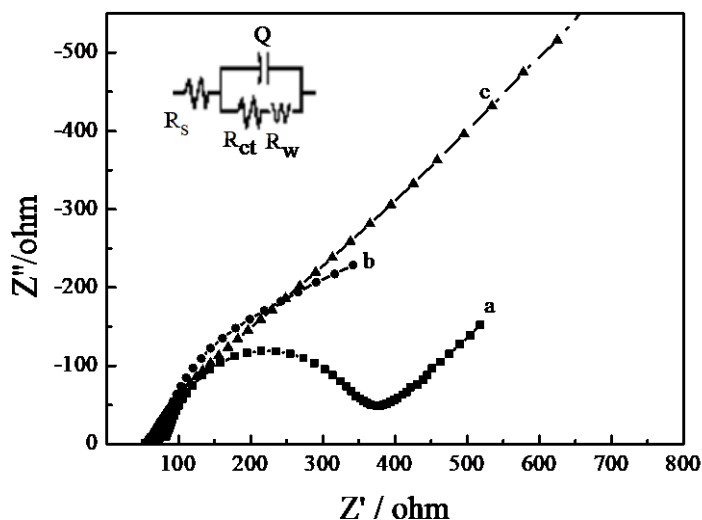


Figure 3. Nyquist diagram (Z'' vs. Z') for the EIS measurements in the presence of 1.0×10^{-3} mol/L $K_3Fe(CN)_6 / K_4Fe(CN)_6$ at bare GCE (a), GR/GCE (b), and GR/PtNPs/GCE (c).

The electrochemical impedance spectroscopy (EIS) was employed to characterize the GR /PtNPs film coated GCE. EIS plots of 1.0×10^{-3} mol/L $Fe(CN)_6^{3-} / Fe(CN)_6^{4-}$ at different electrodes are depicted in Figure 3. The complex plane diagrams (Nyquist plot, Z'' vs. Z') of EIS includes a semicircular portion and a linear portion. The semicircle portion at high frequency zone is due to the charge transfer resistance (R_{ct}) and the linear portion at the low frequency zone corresponds to the

diffusion process. An ignorable semicircle and a large linear area was observed at GR/PtNPs/GCE (c), which demonstrates that the ohmic and kinetic impedance responses of $\text{Fe}(\text{CN})_6^{3-/4-}$ at this modified GCE are smaller than that at the other electrodes (a, b). It is clear that the GR/PtNPs can greatly enhance the electron transfer rate between $\text{Fe}(\text{CN})_6^{3-/4-}$ and the electrode surface. Compared with other electrodes, $\text{Fe}(\text{CN})_6^{3-/4-}$ can transfer easily from liquid film to the active point of this modified electrode surface. This phenomenon may be attributed to the excellent electric capability and large specific surface area of this composite film.

The circuit model of $R(C(RW))$ was chosen to fit the impedance data obtained, which comprises the solution resistance (R_s), the charge transfer resistance (R_{ct}), ion diffusion resistance (R_w) and double-layer capacitance (Q). By fitting the data, R_{ct} was estimated to be 254.2Ω at the GCE (a). The R_{ct} decreased to 146Ω due to the accelerating of electron-transfer by GR (b). On the GR/PtNPs/GCE (c), the R_{ct} further decreased to 57.11Ω , indicating the much lower electron-transfer resistance on the GR/PtNPs/GCE compared with that on GR/GCE. These results may be attributed to the synergic effect of the unique characteristic of GR such as large specific area, strong adsorption ability and the catalytic performance of PtNPs.

3.4 Electrochemical behavior of Trp and Tyr at the different electrodes

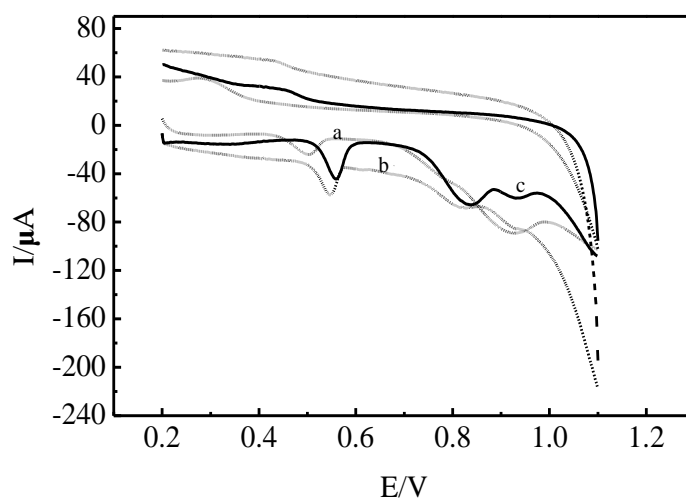


Figure 4. Cyclic voltammetric curves of 3.0×10^{-5} mol/L Trp and 2.0×10^{-5} mol/L Tyr in the presence of 5-HTP at different electrodes at bare GCE (a), GR/GCE (b), and GR/PtNPs/GCE (c).

Voltammetric responses of Trp and Tyr at the different electrodes in the presence of 5-HTP were investigated by cyclic voltammetry (CV), as shown in Figure 4. Within the potential window from 0.2 to 1.1 V, there are two oxidation peaks at bare GCE (curve a). The oxidation peak at 0.503 V is due to voltammetric response of 5-HTP, and the wide peak at 0.929 V corresponds to the oxidation peak of Trp and Tyr, which indicates that the oxidation of Trp and Tyr can't be well separated at bare GCE. Figure 4 illustrates two poor oxidation peaks of Trp and Tyr are respectively recorded at 0.822 V and 0.924 V on GR/GCE (curve b). Simultaneously, two sensitive oxidation peaks were observed at

0.834 V and 0.936 V on GR/PtNPs/GCE, respectively. Compared with that of GR/GCE, the anodic peak currents were enhanced significantly. This phenomenon may be attributed to the collective performance of the unique characteristic of GR and the catalytic characteristics of PtNPs. From the experimental results, GR/PtNPs/GCE can be employed for the simultaneous determination of Trp and Tyr.

3.5 Optimization of the measurement conditions

3.5.1 Optimizing of supporting electrolyte and choice of pH

The electrochemical responses for Trp and Tyr might be affected by the supporting electrolyte solution. Linear sweep voltammetry (LSV) was used to study the influence of some supporting electrolytes on the voltammetric responses of Trp and Tyr, such as Britton-Roinson solution, acetic acid-sodium acetate, disodium hydrogen phosphate-citric acid, citric acid- sodium citrate, hydrochloric acid- potassium acid phthalate and sulfuric acid-sodium sulfate. The results showed that the oxidation peak potentials of Trp and Tyr can be well separated in sulfuric acid- sodium sulfate, however, they are overlapped in other buffer solutions. In addition, the oxidation peaks were closely related to pH value of supporting electrolyte. The effect of solution pH on the oxidation peak was investigated from pH 0.32 – 1.10. With the increment of pH, the peak current increased gradually and achieved a maximum at pH=0.4, therefore, pH=0.40 sulfuric acid- sodium sulfate was chosen as the supporting electrolyte. The separation of the oxidation peak potentials (ΔE_p) for Trp and Tyr reached 100 mV, while at carbon nanofibers modified carbon paste electrode (CNF-CPE), ΔE_p was only 50 mV reported by Tang [21].

3.5.2 Effect of the amount of composite modifier

The amount of GR/PtNPs dispersion on GC electrode directly decides the thickness of GR/PtNPs film, and the latter will influence the voltammetric response of Trp and Tyr. Their oxidation peak currents increased with increasing the amount of GR/PtNPs dispersion from 2 to 6 μL . If further increasing the amount of GR/PtNPs dispersion, the oxidation peak current conversely decreased. This phenomenon is probably that composite film (containing PSS) becomes thicker and blocks the mass transport and electron transfer. So, 6 μL of GR/PtNPs was used for the fabrication of the GR/PtNPs/GCE in all subsequent experiments.

3.5.3 Influence of scan rate

The influence of scan rate on the oxidation peak current ($I_{p,a}$) of Trp and Tyr at GR/PtNPs/GCE was discussed by LSV. The results demonstrated $I_{p,a}$ varied linearly with the increase of scan rate from 20 to 500 mV/s. The linear regression equations of $I_{p,a}$ versus v are as follows:

$$I_p (10^{-5} \text{ A}) = -0.108 + 0.062 v \quad (R=0.9978) \quad (1)$$

$$I_p (10^{-5} \text{ A}) = -0.733 + 6.79v \quad (R=0.9985) \quad (2)$$

They indicate that the electrochemical processes of Trp and Tyr at this modified electrode are adsorption-controlled. These results are in accord with that of the previous reports [22].

3.5.4 Choice of accumulation condition

As an impactful way, accumulation is often employed to raise the sensitivity of the determination, especially for the trace analysis. The influence of accumulation potential on $I_{p,a}$ of Trp and Tyr was investigated at different potentials from 0.6 to 0.7 V. $I_{p,a}$ kept almost constant versus the different potential, which indicates that the accumulation potential has no effect on $I_{p,a}$ of Trp and Tyr. Thus, an open-circuit accumulation was further employed for the determination of Trp and Tyr. The variation of $I_{p,a}$ of Trp and Tyr versus the accumulation time was also discussed. The peak current increased distinctly with increasing accumulation time within 50 s. This phenomenon is probably due to the adsorption of Trp and Tyr on the surface of GR/PtNPs/GCE. However, the peak current decreased slightly after 50 s, implying that the modified electrode was saturated with adsorbed Trp and Tyr.

3.6 Calibration graph

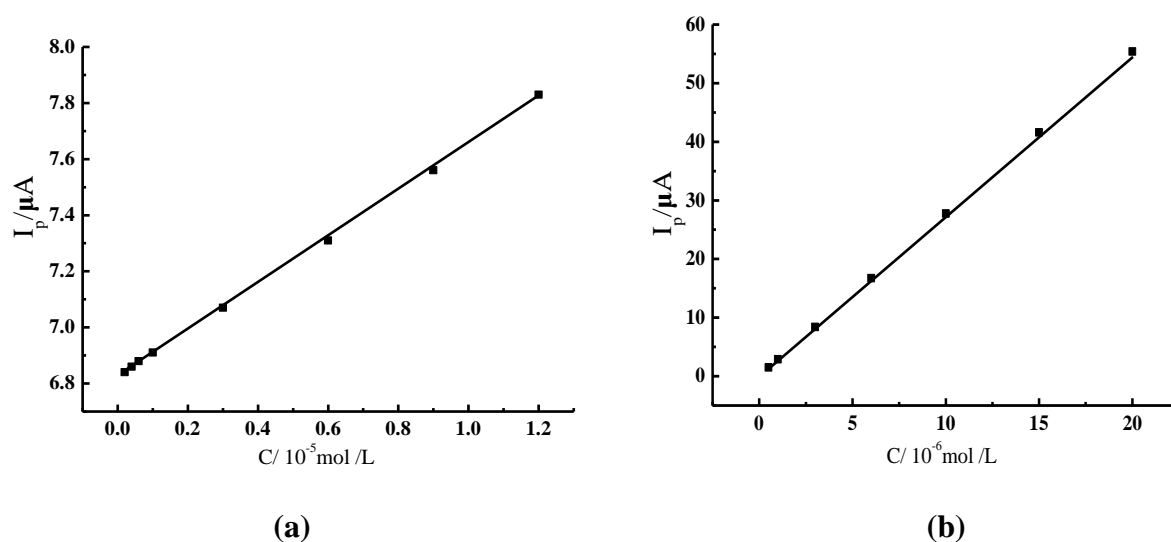


Figure 5. Calibration curves between the peak current and the concentration of Trp (a) and Tyr (b).

Under optimum measurement conditions, the calibration graph about the oxidation peak current with varied concentration of Trp and Tyr in the presence of $3.0 \times 10^{-5} \text{ mol/L}$ 5-HTP was examined by employing LSV. $I_{p,a}$ is proportional to the concentration of Trp from 2.0×10^{-7} to $1.2 \times 10^{-5} \text{ mol/L}$. The detection limit of Trp is estimated to be $8.22 \times 10^{-8} \text{ mol/L}$ according to $S/N = 3$. $I_{p,a}$ varies linearly with the increment of the concentration of Tyr from 5.0×10^{-7} to $2.0 \times 10^{-5} \text{ mol/L}$ with a detection limit of $1.25 \times 10^{-7} \text{ mol/L}$. The experiment results suggest that the developed sensor in this work can be served

as a promising approach for simultaneous determination of Trp and Tyr. The comparison about the performance of some sensors in the detection of Trp and Tyr are summarized in Table 1. As can be seen from Table 1, the detection limit of this work is lower than those of other sensors.

Table 1. Comparison of different sensors for voltammetric determination of Trp and Tyr

Sensors	Linear range for Tyr (μM)	Detection limit for Tyr (μM)	Linear range for Trp (μM)	Detection limit for Trp (μM)	Reference
CNF-CPE	0.2-109	0.1	0.1-119	0.1	[21]
Boron-doped diamond	100-700	1.0	20-1000	10	[23]
NanoAu-MWCNT /GCE			5.0-100	3.0	[24]
ERGO/GCE	0.5-80	0.2	0.2-40	0.1	[25]
SWCNHs/GCE	2.0-30	0.4	0.5-50	0.05	[26]
Nafion/TiO ₂ - GR/GCE	10-160	2.3	5.0-140	0.7	[27]
GR/PtNPs /GCE	0.5-20	0.125	0.2-12	0.082	This work

MWCNT : multi-walled carbon nanotubes, GCE: glassy carbon electrode, ERGO: electrochemically reduced graphene oxide, SWCNHs: single-walled carbon nanohorns, CNF-CPE: carbon nanofiber modified carbon paste electrode, GR: graphene, PtNPs: Pt nanoparticles

3.7 Interferences

Based on the experimental results in section 3.4, 5-HTP has no interference on voltammetric detection of Trp and Tyr. To evaluate the selectivity of the assay of Trp and Tyr, the interferences of other amino acids on the measurement of Trp and Tyr at 2.0×10^{-5} mol/L level was examined. 5-fold concentrations of L-methionine, 10-fold L-lysine, cysteine, aspartic acid, 15-fold L-arginine, L-proline, 25-fold L-leucine, 60-fold L-alanine had no influences on the signals of 2.0×10^{-5} mol/L Trp and Tyr with deviation below 5%. Therefore, this method has good selectivity for the simultaneous detection of Trp and Tyr.

3.8 Reproducibility and stability of composite modified electrode.

Under the optimum condition, 2.0×10^{-5} mol/L Trp and Tyr were measured repeatedly 8 times using GR/PtNPs/GCE. Relative standard deviations (RSD) of the peak currents were 2.43% and 1.38%, which indicate that this sensor has a good reproducibility. The long-term stability of this sensor was also evaluated by LSV within 10 days. GR/PtNPs/GCE was employed to detect Trp and Tyr once every day, and then stored in the air. The results demonstrated that the peak current responses deviated only 2.77% for Trp and 2.08% for Tyr at the tenth day, indicating that the method has long-term stability.

3.9 Simultaneous detection of Trp and Tyr in pharmaceutical formulation

This sensor was used to simultaneously detect the content of Trp and Tyr in two kinds of compound amino acid injections. Under the optimum conditions, the determination of Trp and Tyr was performed by using the method in section 2.4.

Table 2. Measurement of Trp and Tyr in pharmaceutical formulations

Sample	Labeled amount (10^{-4} $\mu\text{g/mL}$)	Detected (10^{-4} $\mu\text{g/mL}$)	Recovery (%, n=6)	Measured by HPLC (10^{-4} $\mu\text{g/mL}$)
Trp 1	9.0	9.11	102.9	9.12
Tyr 1	2.5	2.47	98.4	2.61
Trp 2	4.3	4.37	98.7	4.35
Tyr 2	1.65	1.66	103.5	1.64

The contents of Trp and Tyr are obtained from their regression equations, and the results are listed in Table 2. At the same time, to examine the suitability of this novel method, known amounts of Trp and Tyr were added into sample solution and the same approach was applied. The recoveries are found to be 98.7~102.9% for Trp and 98.4~103.5% for Tyr, suggesting that this method possessed good accuracy. Additionally, high performance liquid chromatograph (HPLC) was also applied to determine Trp and Tyr content to prove the reliability of this method, as shown in Table 2. There is no significant difference between the determination result of this proposed method and that of HPLC by the evaluation of F test [28].

4. CONCLUSIONS

In this work, a composite material of GR/PtNPs was fabricated, and the GR/PtNPs/GCE was developed for voltammetric determination of Trp and Tyr in the presence of 5-HTP. The novel sensor in the simultaneous detection of two amino acids exhibited high sensitivity and good selectivity compared with the bare GCE. The linear plots between the oxidation peak current of Trp and Tyr and their concentration were found. Based on this, a sensitive analytical method for the simultaneous determination of Trp and Tyr in pharmaceutical formulation was proposed. This proposed method possessed the advantages of rapid response, simplicity and high selectivity.

ACKNOWLEDGEMENTS

This research was supported by the grants from the Natural Science Key Foundation of Henan Province Universities of China (No. 17A150038), the Skeleton Teacher Foundation of Henan Province Universities, China (No. 2009GGJS_123).

References

1. M. H. Fernstrom, J. D. Fernstrom Acute, *Life Sci.*, 97 (1995) 57.
2. Q. Xu, S. F. Wang, *Microchim. Acta*, 151(2005) 47.
3. J.B. Raof, R. Ojani, K.M. Hassan, *Electroanalysis*, 20 (2008) 1259.
4. N. Sultana, M. S. Arayne, M.M. Khan, D. M. Saleem, A.Z. Mirza, *J. Chromatogr. Sci.*, 50 (2012) 531.
5. Y. Ishii, M. Lijima, T. Umemura, A. Nishikawa, Y. Iwasaki, R. Ito, K. Saito, M. Hirose, H. Nakazawa, *J. Pharm. Biomed. Anal.*, 41(2006)1325.
6. Y. Huang, X. Jiang, W. Wang, J. Duan, G. Chen, *Talanta*, 70 (2006) 1157.
7. M.Hasani, M.Moloudi, F.Emami, *Anal. Biochem.*, 370 (2007) 68.
8. X. Liu, L. Luo, Y. Ding, Z. Kang, D. Ye, *Bioelectrochemistry*, 86 (2012)38.
9. M.L. Yola, N. Atar, *J. Electrochem. Soc.*, 163 (2016) B718.
10. T. Madrakian, E. Haghshenas, A. Afkhami, *Sens. Actuators, B*, 193 (2014) 451.
11. J. H. Li, D. Z. Kuang, Y. L. Feng, F.X. Zhang, Z. F. Xu, M.Q. Liu, D. P. Wang, *Biosens. and Bioelectron.*, 42 (2013) 198.
12. M. X.Zheng, F.Gao, Q.X.Wang, X.L. Ci, S.L. Jiang, L.Z.Huang, F. Gao, *Mater. Sci. Eng. C*, 33 (2013) 1514.
13. C. Berger, Z.Song, T.X. Li, A.Y.Ogbazghi, R.Feng, A. N. Dai Marchenkov, E.H.Conrad, P.N.First, and W.A.de Heer, *J. Phys. Chem. B*, 108 (2004) 19912.
14. J. Li, J. Yang, Z.J.Yang, Y. F. Li, S.H. Yu, Q. Xu, X.Y. Hu, *Anal. Methods*, 4 (2012) 1725.
15. X.J. Zhu, J. Zhao, T.T. Jia, S.H. Li, N. Li, H.B. Hou, R.L. Zhong, Z. Fan, M.J. Guo, *Carbohydr. Polym.*, 209 (2019) 258.
16. S.Stankovich, R. D.Piner, X.Chen, N.Wu, S. T. Nguyen, R. S. Ruoff, *J. Mater. Chem.*, 16 (2006) 155.
17. M. Q. Yang, X. Zhang, Y. Yan, *Chin. J. Anal. Chem.*, 46 (2018) 1968.
18. G. Saravanan, S. Mohan, *Appl. Surf. Sci.*, 386 (2016) 96.
19. K. P.Liu, J. J.Zhang, G. H.Yang, *Electrochem. Commun.*, 12 (2010) 402.
20. Y. C.Si, E.T. Samulski, *Nano Lett.*, 8 (2008)1679.
21. X. F. Tang, Y. Liu, H.Q. Hou, T.Y. You, *Talanta*, 80 (2010) 2182.
22. S. Güney, G. Yıldız, *Electrochim. Acta*, 57(2011)290.
23. G. H. Zhao, Y. Qi, Y. Tian, *Electroanalysis*, 18 (2006) 830.
24. M. Kooshki, H. Abdollahi, S. Bozorgzadeh, B. Haghghi, *Electrochim. Acta*, 56 (2011) 8618.
25. K. Q. Deng, J.H.Zhou, X.F. Li, *Colloids Surf. B*, 101 (2013) 183.
26. S. Zhu, J. Zhang, X.E. Zhao, H. Wang, G. Xu, J. You, *Microchim. Acta*, 181 (2014) 445.
27. Y. Fan, J. H. Liu, H.T. Lu, Q. Zhang, *Microchim. Acta*, 173 (2011) 241
28. Wuhan University, “*Anal. Chem. (Fifth Edition)*”, Higher Education Press, (2006) Beijing, P. R. China